NADPH oxidase-mediated reactive oxygen species production activates hypoxia-inducible factor-1 (HIF-1) via the ERK pathway after hyperthermia treatment

Eui Jung Moon[a], Pierre Sonveaux[b], Paolo E. Porporato[b,c], Pierre Danhier[b,c], Bernard Gallez[c], Ines Batinic-Haberle[d], Yu-Chih Nien[a], Thies Schroeder[d], and Mark W. Dewhirst[a,d,1]

Departments of [a]Pathology and [d]Radiation Oncology, Duke University Medical Center, Durham, NC 27710; and [b]Unit of Pharmacology and Therapeutics and [c]Unit of Biomedical Magnetic Resonance, University of Louvain Medical School, B-1200 Brussels, Belgium

Edited* by Gregg L. Semenza, The Johns Hopkins University School of Medicine, Baltimore, MD, and approved October 12, 2010 (received for review May 19, 2010)

Hyperthermia (HT) is a strong adjuvant treatment with radiotherapy and chemotherapy because it causes tumor reoxygenation. However, the detailed molecular mechanisms of how HT enhances tumor oxygenation have not been elucidated. Here we report that 1 h of HT activates hypoxia-inducible factor-1 (HIF-1) in tumors and its downstream targets, vascular endothelial growth factor (VEGF) and pyruvate dehydrogenase kinase 1 (PDK1). Consistent with HIF-1 activation and up-regulation of its downstream genes, HT also enhances tumor perfusion/vascularization and decreases oxygen consumption. As a result, tumor hypoxia is reduced after HT, suggesting that these physiological changes contribute to HT-induced tumor reoxygenation. Because HIF-1 is a potent regulator of tumor vascularization and metabolism, our findings suggest that HIF-1 plays a role in HT-induced tumor reoxygenation by transactivating its downstream targets. We demonstrate that NADPH oxidase-mediated reactive oxygen species production, as a mechanism, up-regulates HIF-1 after HT. Furthermore, we determine that this pathway is initiated by increased transcription of NADPH oxidase-1 through the ERK pathway. In conclusion, this study determines that, although HIF-1 is a good therapeutic target, the timing of its inhibition needs to be optimized to achieve the most beneficial outcome when it is combined with other treatments of HT, radiation, and chemotherapy.

Hyperthermia (HT) has been investigated for its propensity to induce tumor reoxygenation (1, 2). When tumors are subjected to temperatures between 39 °C and 43 °C, improvements in oxygenation have been observed both during and up to 24 h after heating. This temperature range is referred to as mild HT because direct cytotoxicity is minimal in this range (3). Various clinical trials have confirmed that mild HT induces tumor reoxygenation at 24 h after HT in cancer patients (4–7) and that reoxygenation is associated with better patient treatment outcome. In addition, mild HT is being used with thermally sensitive liposomes containing doxorubicin as a unique method to enhance tumor-specific drug delivery (8–10). Because of these benefits, mild HT is a promising adjuvant treatment to target tumor hypoxia.

Mild HT-induced tumor reoxygenation is known to be caused by enhanced oxygen delivery (11) and decreased oxygen consumption (12–15). However, the molecular mechanisms that control these physiological changes are unknown. Hypoxia-inducible factor-1 (HIF-1) is a potent mediator of hypoxic responses by regulating both oxygen delivery (angiogenesis) and oxygen consumption (glycolytic metabolism) (16–18). Therefore, in this study, we sought to determine whether HIF-1 plays a role in HT-induced tumor reoxygenation.

As a transcription factor, HIF-1 is known to activate more than 60 target genes involved in solid tumor progression (19). It is highly expressed in most tumor types, and its expression has been correlated with poor patient outcome (19–21). The functional HIF-1 is composed of α- and β-subunits. Unlike the constitutively expressed HIF-1β subunit, HIF-1α stabilization is usually regulated by prolyl hydroxylase (PHD)-mediated proteasomal degradation (22). PHD requires oxygen, 2-oxoglutarate, and iron to hydroxylate the oxygen-dependent degradation (ODD) domain of HIF-1α. A lack of oxygen, metabolic intermediates, or iron inhibits PHD activity and stabilizes HIF-1α. When stabilized, HIF-1α forms a heterodimer with HIF-1β and binds to the hypoxia response element to transactivate the expression of many downstream genes involved in tumor progression, including angiogenesis [vascular endothelial growth factor (VEGF) (23)] and glycolytic metabolism [PDK1 (24)].

The effect of heat on HIF-1 has been reported previously in several studies. Although 1 h of heat treatment down-regulates HIF-1α and VEGF levels in murine macrophages under hypoxia (25), in tumor cells heat increases HIF-1α independently of oxygen (26, 27). However, the downstream effects of HT-induced HIF-1α up-regulation have not been fully validated. Because HIF-1 plays an important role in tumor vascularization and metabolism, we hypothesize that HIF-1 is involved in tumor reoxygenation after HT.

To test our hypothesis, we address the following questions: (*i*) whether and how HIF-1 is regulated by HT and (*ii*) whether HIF-1 plays a role in HT-induced tumor reoxygenation. The findings in this study provide an important rationale for the development of therapeutic strategies to combine mild HT and HIF-1 inhibition with radiation and chemotherapy.

Results

HT Up-Regulates HIF-1 Expression and Enhances VEGF Secretion in Tumor Cells. To determine the effect of heat on HIF-1, 4T1 mouse mammary carcinoma cells were treated at a series of temperatures for 1 h, a clinically relevant duration of HT. After treatment, HIF-1 activity was detected by HIF-1–specific ELISA. HIF-1 activation was increased significantly at temperatures between 41 °C and 44 °C , the temperature range of mild HT (Fig. 1A). Significant cytotoxic effect was observed only at 44 °C (Fig. S1*A*). Because activation of HIF-1 was highest at 43 °C, we focused our study on HT at this temperature. We also determined whether HIF-1α protein expression is up-regulated using Western blot (Fig. 1*B*). Although kinetics were not the same, HT at 43 °C increased HIF-1α expression as hypoxia treatment did (0.5% O_2 for 24 h). We also confirmed that HT at 43 °C induced HIF-1α up-regulation in other tumor cell lines: MDA-MB-231, a human breast cancer cell line, and SiHa, a human cervix cancer cell line. As to the time course of HT-induced HIF-1 up-regulation, we found that increased HIF-1α

Author contributions: E.J.M., P.S., and M.W.D. designed research; E.J.M., P.S., P.E.P., P.D., and Y.N. performed research; B.G., I.B., and T.S. contributed new reagents/analytic tools; E.J.M., P.S., P.E.P., P.D., and M.W.D. analyzed data; and E.J.M. and M.W.D. wrote the paper.

The authors declare no conflict of interest.

*This Direct Submission article had a prearranged editor.

[1]To whom correspondence should be addressed. E-mail: mark.dewhirst@duke.edu.

This article contains supporting information online at www.pnas.org/lookup/suppl/doi:10.1073/pnas.1006646107/-/DCSupplemental.

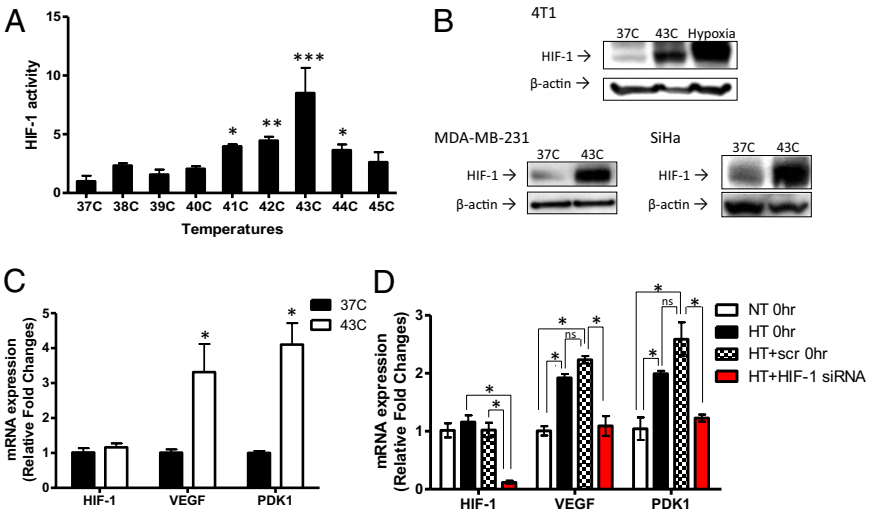

Fig. 1. Heat-induced up-regulation of HIF-1 in tumor cells. (*A*) 4T1 mouse mammary carcinoma cells were HT-treated at temperatures ranging from 37 °C to 45 °C for 1 h. Nuclear extracts were collected and HIF-1 activity was assessed using ELISA. ELISA data were normalized to the mean value of the treatment at 37 °C (mean ± SD, $n = 3$, $^*P < 0.05$, $^{**}P < 0.01$, $^{***}P < 0.005$). (*B*) 4T1 cells were treated with HT (43 °C for 1 h) or hypoxia (0.5% O_2 for 24 h). Two human tumor cell lines, MDA-MB-231 human breast cancer cells and SiHa human cervix cancer cells, were also HT-treated for 1 h at 43 °C. Western blots were performed using whole-cell lysates to detect protein expression of HIF-1α and β-actin. (*C*) After 1 h HT at 43 °C, mRNA expression of HIF-1α and its target genes, VEGF and PDK1, was assessed by qPCR in 4T1 cells (mean ± SD, $n = 3$, $^*P < 0.05$). (*D*) HIF-1–mediated regulation of VEGF and PDK1 mRNA expression was determined by qPCR with or without knocking down HIF-1α in MDA-MB-231 cells. Cells were transfected with SMARTpool siRNA specifically targeting HIF-1α and HT-treated 48 h after transfection (mean ± SD, $n = 3$, $^*P < 0.005$; ns: not significant).

expression in the HT group remained elevated at 6 h post-HT and decreased to a level similar to the control group 24 h after HT (Fig. S1*B*).

As mentioned above, HIF-1 transactivates multiple categories of genes to promote tumor growth, including VEGF, one of the most potent angiogenic factors, and PDK1, a metabolic enzyme that converts tumor metabolism to glycolysis by inactivating the tricarboxylic acid (TCA) cycle enzyme, pyruvate dehydrogenase (PDH). To further investigate whether HT-induced HIF-1 could up-regulate VEGF and PDK1, we determined their mRNA expression by quantitative real-time reverse transcriptase PCR (qPCR) immediately after HT treatment (Fig. 1*C*). One hour of HT at 43 °C significantly increased mRNA expression of VEGF and PDK1 in 4T1 cells (three- to fourfold), but did not change HIF-1α mRNA expression. This result indicates that HT regulates HIF-1α expression at the post-transcriptional level.

HT also increased mRNA expression of VEGF and PDK1 in MDA-MB-231 cells (Fig. 1*D*). Furthermore, knocking down HIF-1α using SMARTpool siRNA (Fig. S1*C*) abrogated the increase in VEGF and PDK1 mRNA expression following HT (Fig. 1*D*). These findings suggest that HT-induced transcription of VEGF and PDK1 is specifically mediated by HIF-1.

Because VEGF is a secreted protein (28), we next examined whether up-regulated VEGF mRNA expression could lead to increased VEGF secretion after HT. VEGF ELISA demonstrated that HT significantly increased VEGF secretion by 4T1 tumor cells at 6 and 24 h after HT in comparison with controls at the same time points (Fig. S1*D*).

Heat Activates HIF-1 and VEGF in Tumors in Vivo. To evaluate HT-induced HIF-1α expression serially and noninvasively in vivo, we used a previously established HIF-1α reporter cell line, 4T1-ODD-Luc (29). This cell line contains a luciferase reporter gene fused with the HIF-1α ODD domain, allowing direct visualization of HIF-1α protein stability. Subcutaneously grown 4T1-ODD-Luc tumors were locally HT-treated, and HIF-1α reporter activity was monitored at various time points after HT treatment. Compared with the control, HIF-1α reporter activity significantly increased immediately after HT (0 h). It peaked at 6 h post-treatment and decreased to the levels of the control 48 h after HT (Fig. 2*A* and *B*). Consistent with HIF-1α reporter activity, HIF-1 ELISA data showed that HIF-1 activation was also significantly increased 6 h after HT in tumor tissues (Fig. S2*A*). We further measured VEGF levels in mouse tumor tissues 6, 24, and 48 h after HT. ELISA and immunohistochemistry demonstrated significant increases in VEGF levels 48 h after HT (Fig. 2*C* and Fig. S2 *B* and *C*). These findings provide direct evidence that HT up-regulates the expression of both HIF-1α and its downstream target, VEGF, in vivo.

As it was observed in cells, necrotic areas in HT-treated tumor tissues were not significantly different from the control (Fig. S2*D*). In fact, the necrotic fraction is lower in the HT group at 48 h than in the controls. Therefore, decreased tumor hypoxia after HT does not seem to be a result of the cell-killing effect.

HT Promotes Tumor Perfusion/Vascularization, Decreases Oxygen Consumption, and Down-Regulates Tumor Hypoxia. Consistent with increases in tumor tissue VEGF levels, tissue staining with the endothelial marker CD31 demonstrated a significant increase in the number of tumor blood vessels 48 h after HT (Fig. 3*A*). These

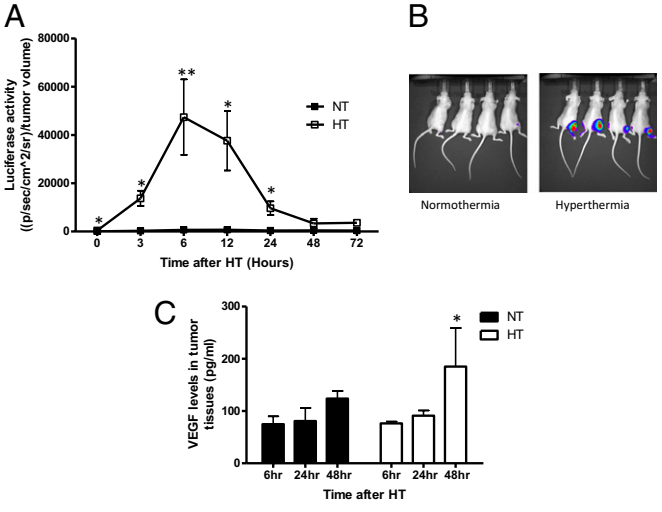

Fig. 2. HT-induced activation of HIF-1 in vivo. (*A*) To noninvasively monitor HIF-1α expression in vivo, the reporter cell line, 4T1-ODD-Luc (29), was injected subcutaneously into the right flank of nude mice. Mice were HT-treated using a preheated water bath for 1 h and imaged at various time points after treatment. Compared with the normothermic group, activity of the HIF-1α reporter was significantly increased immediately after HT and peaked at 6 h following treatment (NT: normothermia, HT: hyperthermia; mean ± SEM, $n = 8$, $^*P < 001$, $^{**}P < 0.005$). Elevated HIF-1α reporter activity decreased to the levels of the control treatment within 48 h. (*B*) Activation of the ODD-luciferase reporter was noninvasively imaged using the Xenogen IVIS bioluminescence imaging system (Representative images were taken at 6 h after HT.) (*C*) VEGF protein levels in tumor tissues were determined using ELISA. Forty-eight hours after treatment, VEGF production was significantly increased in the HT group compared with the control (mean ± SEM, $n = 5$, $^*P < 0.05$).

data suggest that HT induces more robust tumor angiogenesis than the control treatment. At the same time point, we also observed significantly increased tumor perfusion from HT-treated tumor tissues using the perfusion marker Hoechst 33342 (Fig. 3*B*). Further analysis of the spatial distribution of tumor vasculature demonstrated that about 70% of tumor vessels were located in the perfused areas 48 h after HT (Fig. S3*A*). In contrast, only 30% of total tumor vessels were located in perfused areas in control tumors. These findings suggest that HT not only improves overall tumor perfusion but also stimulates perfused blood vessel formation. Because VEGF is a pivotal factor for both angiogenesis and vessel perfusion, the temporal concordance in HT-induced HIF-1α up-regulation, enhanced VEGF levels, and stimulated angiogenesis as well as improved tumor perfusion reveals a series of multifaceted physiological changes in the tumor microenvironment after HT. Because our previous study showed that HIF-1 induces robust angiogenesis over a 24- to 48-h time frame, the result here is not unexpected (31).

Previous studies suggested that, in addition to increased oxygen delivery, decreased oxygen consumption may induce tumor reoxygenation after HT (1, 2, 12–15). Observations of increased tumor tissue accumulation of lactate (12, 13) and decreased mitochondrial function in tumor cells after HT (14) indicate that the metabolic switch from oxidative phosphorylation to glycolysis may potentially decrease tumor oxygen consumption. To directly determine the effects of HT on tumor oxygen consumption, we measured tumor cell oxygen consumption rates using electron paramagnetic resonance (EPR) oximetry (32). Compared with 37 °C treatment (slope: −2.035 ± 0.097), 1 h of HT significantly reduced oxygen consumption rates in 4T1 cells by 30% (slope: −1.404 ± 0.073, Fig. 3*C*). In contrast to decreased oxygen consumption rates, tumor ATP levels remained unchanged in vitro (Fig. S3*B*) and in vivo (Fig. S3*C*), indicating that ATP production is maintained by increased glycolysis. We also found a significant increase in mouse plasma lactate levels 6 h after HT (Fig. S3*D*). This observation also supports the switch to a glycolytic metabolism. No significant changes in mouse plasma lactate levels were observed at later time points of 24 and 48 h post-treatment. Because we observed an increase in PDK1 mRNA expression after HT, we examined whether HIF-1–regulated PDK1 is involved in decreased oxygen consumption rates by altering tumor metabolism toward glycolysis. PDK1 was knocked down using PDK1-specific shRNA (Fig. S4*A*) and tumor cell oxygen consumption rates were measured. As observed previously (Fig. 3*C*), HT significantly decreased tumor oxygen consumption rates by 46% (slope: −1.625 ± 0.034) compared with the control treatment at 37 °C (slope: −3.031 ± 0.031). Although it was statistically significant (43 °C scrambled vs. 43 °C PDK1 shRNA, $P < 0.0001$), PDK1 depletion partially blocked the decrease in oxygen consumption rates by 15% (slope: −1.877 ± 0.033; Fig. S4 *A* and *B*) compared with the scrambled control. We also observed that mitochondrial membrane potential was significantly decreased after HT, suggesting that decreased oxygen consumption rates are caused by both a HIF-1–mediated increase in PDK1 and a direct effect of HT on mitochondria (Fig. S4*C*).

Next, to determine whether the enhanced tumor perfusion/vascularization and decreased oxygen consumption rates after HT could affect tumor hypoxia, we assessed tumor tissues by immunostaining with a hypoxia-specific marker, EF5 (30). Hypoxic areas of tumors were significantly decreased 24 and 48 h after HT (Fig. 3*D* and Fig. S4*D*). Therefore, decreased tumor hypoxia at 24 and 48 h after HT possibly mirrors the changes in tumor physiology of both enhanced perfusion/vascularization and reduced oxygen consumption.

Reactive Oxygen Species Play a Role in HT-Induced HIF-1 Up-Regulation. It has been shown that hypoxia is a potent factor enhancing HIF-1α expression (33). However, our findings above demonstrate that HT-induced HIF-1α stabilization occurs in less hypoxic conditions and even in normoxic environments. To elucidate the mechanism of this non-hypoxia–induced HIF-1α accumulation, we next investigated whether other factors independent of oxygen availability may up-regulate HIF-1α. We previously reported that reactive oxygen species (ROS) contribute to HIF-1 activation after radiation (34). Thus, we examined whether ROS play a role in HT-mediated HIF-1α up-regulation. Flow cytometry analysis using a fluorescent dye, CM-H_2DCFDA, demonstrated that HT at 43 °C causes a significant increase in ROS production in 4T1 cells (Fig. 4A). The elevated ROS levels returned to the levels in the control cells within 24 h after HT, which was consistent with HIF-1 up-regulation (Fig. S5*A*). Additionally treating cells with a Mn-porphyrin–based SOD mimic and peroxynitrite scavenger, Mn(III) meso-tetrakis(*N*-ethylpyridinium-2-yl)porphyrin (MnTE-2-PyP5+) (35), inhibited HIF-1α up-regulation after HT, suggesting that ROS are responsible for HIF-1 up-regulation after HT (Fig. S5*B*).

It was separately reported that ROS produced from either mitochondria (36) or NADPH oxidase (37) are responsible for HIF-1α stabilization under hypoxic conditions. To examine whether NOX1 or cytochrome C are involved in HT-induced ROS production and up-regulation of HIF-1α, their mRNA expression was assessed after HT using qPCR. Experiments were

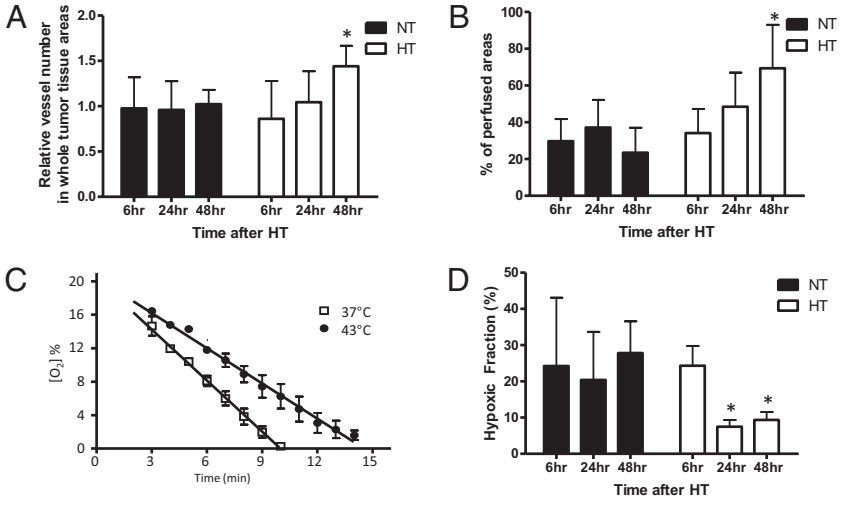

Fig. 3. Changes in tumor physiology result in increased tumor perfusion/vascularization, reduced oxygen consumption rates, and decreased hypoxia after HT. (*A*) Tumor tissues were excised 6, 24, and 48 h after HT. Tumor tissues were cut into 10-μm sections and stained with the endothelial marker CD31. The number of CD31-positive blood vessels in the viable tumor tissue area was counted. Compared with the control treatment, it was significantly increased 48 h after HT (mean ± SEM, $n = 5$, $^*P < 0.05$). (*B*) Perfused areas in 4T1 tumor tissues were determined by imaging the preinjected perfusion marker Hoechst 33342. The percentage of perfused areas to viable tumor areas was significantly increased 48 h after HT compared with the control group (NT: normothermia, HT: hyperthermia, mean ± SEM, $n = 5$, $^*P < 0.05$). (*C*) After HT, tumor oxygen consumption rates were measured in 4T1 cells using EPR oximetry. Oxygen consumption rates were calculated from the slope of the change in oxygen concentration with time. Compared with the control treatment (slope: −2.035 ± 0.097, $n = 4$), the oxygen consumption rates were significantly reduced after HT at 43 °C (slope: −1.404 ± 0.073, $n = 3$, mean ± SD, $^*P < 0.005$). (*D*) Hypoxia in tumor tissues was imaged by probing with a Cy3-conjugated anti-EF5 antibody (ELK3-51) to a preinjected hypoxia marker, EF5 (30). Hypoxic areas of tumors were significantly decreased 24 and 48 h after HT compared with the control treatment (mean ± SEM, $n = 5$, $^*P < 0.005$).

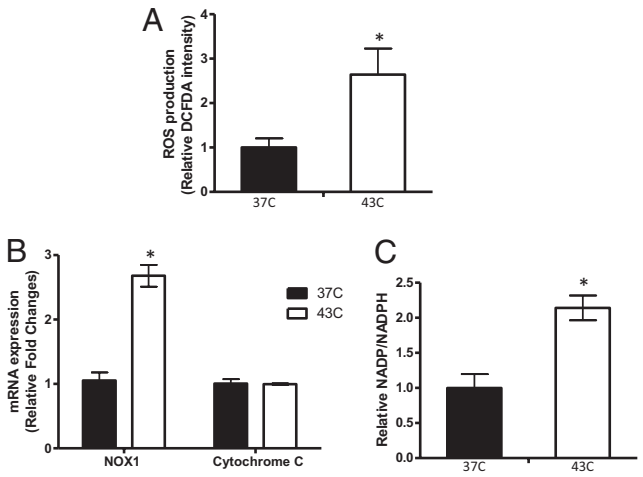

Fig. 4. HT-induced ROS production and NADPH oxidase activation. (*A*) In 4T1 cells, ROS production after HT was measured using the fluorescent dye CM-H_2DCFDA. Fluorescence intensity was normalized to values from the control (37 °C). Compared with the control, HT at 43 °C significantly enhanced ROS production (mean ± SD, $n = 3$, $^*P < 0.05$). (*B*) mRNA expression of NOX1 and cytochrome C was determined immediately after HT in MDA-MB-231 cells. Compared with cytochrome C mRNA, which did not show a significant change, HT at 43 °C significantly increased NOX1 mRNA levels (mean ± SD, $n = 3$, $^*P < 0.005$). Data are representative of three independent experiments. (*C*) The ratio of NADP+/NADPH was determined to evaluate NADPH oxidase activity in MDA-MB-231 cells. HT significantly increased the NADP+/NADPH ratio (mean ± SD, $n = 3$, $^*P < 0.05$).

performed using MDA-MB-231 because this cell line is known to express NOX1 (38). After HT, we found a significant increase in NOX1 mRNA expression in MDA-MB-231 cells, although there was no significant change in cytochrome C mRNA expression (Fig. 4*B*). NADPH oxidase converts NADPH to $NADP^+$ while generating ROS (39). To further investigate whether increased NOX1 mRNA expression leads to enhanced NADPH oxidase activity, we evaluated the $NADP^+$/NADPH ratio. Consistent with an increase in NOX1 mRNA, the $NADP^+$/NADPH ratio was elevated after HT, suggesting that HT activates NADPH oxidase through NOX1 up-regulation (Fig. 4*C*).

To test whether HT affects other subunits of NADPH oxidase, we assessed mRNA expression of p22phox, which is membrane-bound, and of p67phox, which is cytosolic (39). Compared with NOX1, there were no significant changes in their mRNA expression after HT (Fig. S5*C*).

To further determine whether NOX1 is responsible for HT-induced ROS production and HIF-1α activation, we knocked down NOX1 and cytochrome C using SMARTpool siRNA. qPCR confirmed the inhibition of both NOX1 mRNA expression (60% reduction; Fig. S5*D*) and cytochrome C (70% reduction; Fig. S5*E*). After HT, we observed that NOX1 knockdown, but not cytochrome C knockdown, significantly inhibited ROS production (Fig. 5*A*). NOX1 knockdown also reduced HT-induced HIF-1α up-regulation (Fig. 5*B*). In contrast, cytochrome C knockdown did not affect the HIF-1α protein expression after HT. As a result, NOX1 knockdown significantly decreased HT-induced mRNA expression of VEGF and PDK1 to levels of the control (Fig. 5*C*). These findings suggest that NOX1 is required for HT-induced ROS production and HIF-1α accumulation as well as for up-regulation of HIF-1 downstream targets. Again, no changes in HIF-1α mRNA expression were observed in cells with cytochrome C knockdown and NOX1 knockdown, showing that the HIF-1 effects were post-transcriptional.

HT Activates NADPH Oxidase via the ERK Pathway. In Ras-transformed cells, NOX1 transcription is enhanced by the ERK pathway (40). Because it was previously shown that heat shock activates the ERK pathway (41, 42), we investigated whether HT regulates NOX1 and NADPH oxidase through the ERK pathway. In MDA-MB-231 cells, the p38 and JNK pathways showed high basal activation even at 37 °C, and HT did not further enhance their activation (Fig. 6*A*). On the other hand, the ERK pathway was transiently activated by the end of HT (0 h) and returned to baseline 6 and 24 h post-treatment (Fig. 6*A*). To test whether HT-induced ERK activation specifically regulates NOX1 transcription, we suppressed the ERK pathway using U0126, an inhibitor of the upstream ERK regulator, MEK1/2 (43). We treated cells with 500 nM of U0126, which is sufficient to down-regulate ERK activation to basal levels without nonspecific effects (Fig. S6*A*). U0126 treatment abrogated the HT-induced up-regulation of NOX1 mRNA expression (Fig. 6*B*), NADPH oxidase activity ($NADP^+$/NADPH ratio) (Fig. 6*C*), and ROS production (Fig. 6*D*). As a result, HIF-1α expression was suppressed by U0126 (Fig. S6*B*). These findings indicate that NOX1-derived ROS production is mediated by the ERK signaling pathway in response to HT.

Discussion

HT is a strong adjuvant treatment due to its tumor reoxygenation effect. In this study, we demonstrate that HT activates HIF-1 through NADPH oxidase-mediated ROS production and that this pathway is initiated by the ERK pathway. Also, we suggest that activated HIF-1 is involved in tumor reoxygenation by

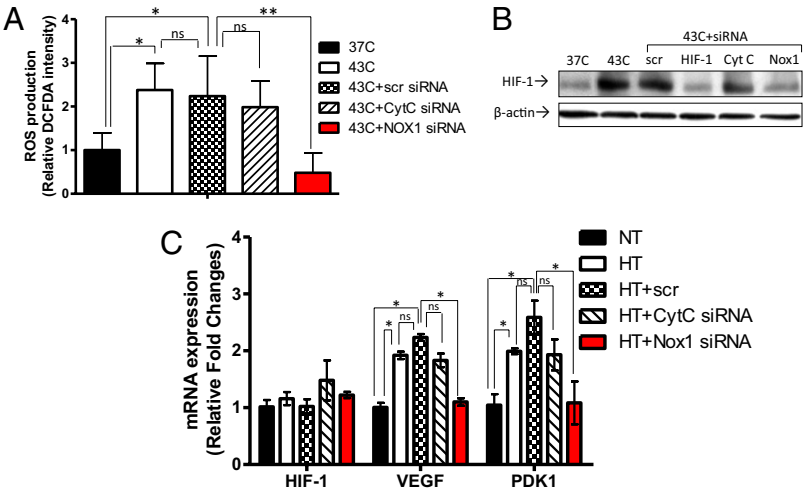

Fig. 5. NADPH oxidase-mediated ROS production and HIF-1 activation. (*A*) To determine the source of ROS production, cytochrome C (CytC) and NOX1 were knocked down in MDA-MB-231 cells using SMARTpool siRNA. After HT, ROS production in NOX1 knockdown cells was significantly decreased, whereas the change was not significant in cytochrome C knockdown cells (mean ± SD, $n = 3$, $^*P < 0.01$, $^{**}P < 0.001$; ns: not significant, scr: scrambled). (*B*) HIF-1α protein expression in MDA-MB-231 cells was determined by Western blot after knocking down cytochrome C or NOX1. Whereas cytochrome C knockdown cells did not affect HT-induced HIF-1α expression, NOX1 knockdown cells showed inhibited up-regulation of HIF-1α after HT. (*C*) Using qPCR, mRNA expression of HIF-1α and its target gene, VEGF, was assessed in wild-type MDA-MB-231 cells or in cells with cytochrome C or NOX1 knockdown. Compared with cells transfected with the cytochrome C targeting siRNA, the HT-induced increase in VEGF mRNA expression was significantly abrogated in NOX1 knockdown cells (mean ± SD, $n = 3$, $^*P < 0.005$; ns: not significant, scr: scrambled).

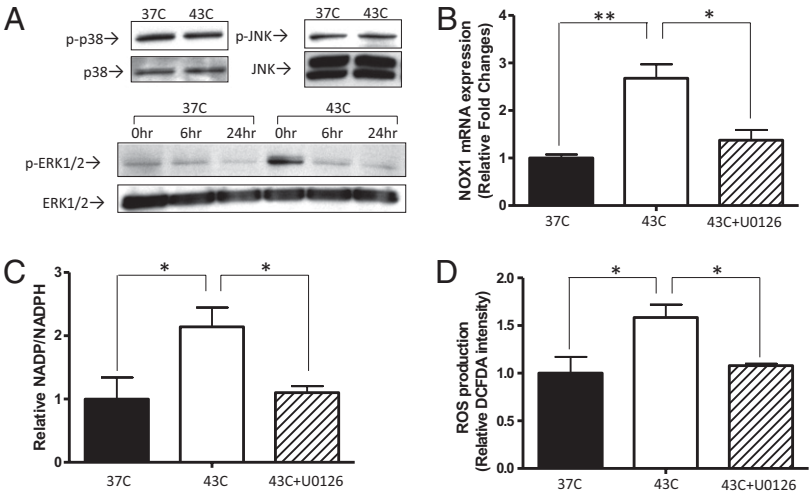

Fig. 6. Regulation of NADPH oxidase through the ERK pathway. (*A*) After HT, the phosphorylation of MAP kinases was assessed by Western blot. Whereas p38 and JNK, which showed high basal activation in MDA-MB-231 cells, were not further phosphorylated by HT, ERK 1/2 was phosphorylated immediately after HT (0 h). Phosphorylation of the ERK 1/2 returned to basal levels at later time points (6 and 24 h after HT). (*B*) In MDA-MB-231 cells, inhibition of the ERK pathway using 500 nM of U0126 significantly inhibited HT-induced up-regulation of NOX1 mRNA levels (mean ± SD, $n = 3$, $^*P < 0.0005$, $^{**}P < 0.0001$), which were measured by qPCR. (*C*) With and without 500 nM of U0126, the $NADP^+$/NADPH ratio was measured after HT. Inhibition of the ERK pathway abrogated the HT-induced activation of NADPH oxidase (mean ± SD, $n = 3$, $^*P < 0.05$). (*D*) ROS production of MDA-MB-231 cells after HT with or without U0126 was determined using the fluorescent dye CM-H_2DCFDA. Inhibition of the ERK pathway inhibited ROS production after HT (mean ± SD, $n = 3$, $^*P < 0.05$).

promoting tumor perfusion/vascularization and partially by decreasing oxygen consumption (Fig. S7).

In this study, we determine that HT stabilizes HIF-1α, leading to increases in VEGF and PDK1 expression in tumors. Up-regulation of these target genes is highly involved in tumor angiogenesis and metabolism, indicating that HT-induced HIF-1 may play important roles in multiple changes in tumor physiology. We show that HT significantly promotes tumor angiogenesis and increases VEGF levels in tumors (Fig. 2*C* and Fig. 3*A*). More interestingly, we further demonstrate that most of these neovessels are located in perfused areas (Fig. S3*A*). Thus, this study suggests that oxygen delivery may possibly be increased through these vessels and cause tumor reoxygenation. To validate functionality and maturity of these vessels, further studies are still required.

In addition to enhanced perfusion/vascularization, we suggest that decreased tumor cell oxygen consumption contributes to tumor reoxygenation after HT (Fig. 3*C*). PDK1 is involved in altering tumor metabolism to glycolysis by inhibiting PDH. Inhibition of PDK1 results in increased oxygen consumption rates (44) and decreased lactate production (45) under hypoxia. However, knocking down PDK1 with shRNA only partially blocked the decrease in tumor cell oxygen consumption rates after HT. Because we also observed that HT decreased mitochondrial membrane potential, these findings suggest that HT regulates oxygen consumption rates both by directly affecting mitochondria and by increasing PDK1 via HIF-1. Therefore, decreased tumor hypoxia at 24 and 48 h post treatment (Fig. 3*D*) corroborates that HT-induced tumor oxygenation is induced by both enhanced oxygen delivery and reduced oxygen consumption.

In addition to the downstream effects of HT-induced HIF-1 activation, we demonstrate that NADPH oxidase-mediated ROS production stabilizes HIF-1α. Previously, our group showed that ROS are involved in radiation-induced HIF-1 activation (34). Inhibition of ROS using a SOD mimic, a small molecule that scavenges ROS (46), inhibits radiation-induced HIF-1 activation and, as a result, sensitizes tumor microvessels to radiation damage. Studies by other groups further reported that ROS are required for HIF-1α stabilization even under hypoxia (36, 37). Each of these studies suggests two sources of ROS as HIF-1 regulators: mitochondria (36) and NADPH oxidase (37). For these, we found that NADPH oxidase-derived ROS production is required for HIF-1 activation in HT-treated cells (Fig. 5 *A* and *B*). We further showed that HT enhances NADPH oxidase activity via the ERK pathway (Fig. 6). Inhibition of the ERK pathway using the specific inhibitor U0126 results in decreased NADPH oxidase activity, ROS production, and HIF-1α expression. These findings not only present important clues to understanding how HT regulates tumor reoxygenation, but also provide a molecular mechanism and therapeutic rationale for the inhibition of HIF-1.

HIF-1 is often considered a promising therapeutic target (19, 20). However, our findings suggest that HIF-1 inhibition needs to be carefully regulated to achieve optimal therapeutic effects. Because hypoxic tumors exhibit both radioresistance and chemoresistance due to increased DNA damage repair and poor drug delivery and drug diffusion (47), combined treatment with HT synergizes treatment outcome by overcoming these limitations. Because mild HT promotes tumor oxygenation, it is more effective if mild HT is administered before radiation and chemotherapy. Meanwhile, HT-regulated induction of HIF-1 activity could be either beneficial or detrimental. Although we suggest that HT-induced HIF-1 up-regulation may play a role in regulating tumor reoxygenation, its possible involvement in drug resistance by up-regulating p-glycoprotein was also reported by Wartenberg et al. (27). Thus, to preferentially take advantage of HT-induced HIF-1 activation and also suppress its deleterious effects, further studies are needed to investigate how HIF-1 activation is regulated by combined treatments of HT, radiation, and chemotherapy. Because our previous study (34) and studies by other groups (48–52) showed that HIF-1 is up-regulated by radiation and chemotherapy, it is possible that combined treatments increase HIF-1 activation to a higher degree than a single treatment. Although enhanced tumor reoxygenation after HT may radiosensitize tumor cells and promote drug delivery, elevated HIF-1 levels may turn on other HIF-1–regulated mechanisms of tumor cell resistance and aggressiveness. Therefore, it is crucial to understand how tumor cells respond to more clinically relevant treatment combinations and how to target HIF-1 in a time-sensitive manner.

In conclusion, our study demonstrates that HT activates HIF-1 through ERK-NADPH oxidase-mediated ROS production, and this enhances tumor oxygenation by up-regulating HIF-1 target genes involved in tumor perfusion/vascularization and metabolism (Fig. S7). These findings suggest that HIF-1 may play a beneficial role in radiosensitizing tumors after HT, and combined administration of HT and HIF-1 inhibitors in a well-optimized manner with conventional treatments could yield an important therapeutic benefit.

Materials and Methods

A detailed description is available in *SI Materials and Methods*.

Briefly, HT treatment was performed using preheated water baths for both in vitro and in vivo studies. In vivo bioluminescence imaging was performed using the Xenogen IVIS bioluminescence imaging system to detect ODD-luciferase signals in mouse tumors. Immunohistochemistry was performed following previously reported procedures (53–55). Tumor oxygen consumption rates were measured by EPR oximetry. ROS production was measured by staining cells with 5-(and-6)-chloromethyl-2′,7′-dichlorodihydrofluorescein diacetate, acetyl ester (CM-H_2DCFDA; Invitrogen). mRNA knockdown was performed by transfecting cells with SMARTpool siRNA (Dharmacon) against

human HIF-1α, NOX1, cytochrome C, or nontargeting control using lipofectamine RNAiMAX (Invitrogen) according to the manufacturer's protocol.

ACKNOWLEDGMENTS. We thank Dr. C. Li (University of Colorado School of Medicine, Aurora, CO) for his generous gift of the 4T1-ODD-Luc cell line; Dr. C. Koch (University of Pennsylvania, Philadelphia) for EF5- and Cy3-conjugated anti-EF5 antibody (ELK3-51); Dr. M. Cook and Dr. T. Dissanayake for their expertise in flow cytometry; and E. Beneteau for excellent technical assistance (University of Louvain Medical Center, Brussels). We also thank J. Kim, H. Rho, Dr. Y. Cao, Dr. J. T. A. Chi, Dr. D. R. Fels, Z. N. Rabbani, Dr. T. Robinson, K. M. Kennedy, C. D. Landon, and A. S. Betof (Duke University, Durham, NC) for their helpful discussions and comments in the preparation of this manuscript. This study was supported by National Institutes of Health Grant P01CA42745-20, -21, and -22; Department of Defense Breast Cancer Research Program Predoctoral Traineeship Awards W81XWH-05-1-0294; Alaska Run For Women Grant SPS142854; the European Research Council FP7/2007-2013 ERC Independent Researcher Starting Grant 243188 TUMETABO; Action de Recherche Concertée ARC 09/14-020 from the Communauté Française de Belgique; and the Fondation Belge Contre le Cancer (200-2008). P.S. is a Research Associate and P.D. is a Research Fellow of the Fonds National de la Recherche Scientifique.

1. Song CW, Park H, Griffin RJ (2001) Improvement of tumor oxygenation by mild hyperthermia. *Radiat Res* 155:515–528.
2. Vujaskovic Z, Song CW (2004) Physiological mechanisms underlying heat-induced radiosensitization. *Int J Hyperthermia* 20:163–174.
3. Oleson JR (1995) Eugene Robertson Special Lecture. Hyperthermia from the clinic to the laboratory: A hypothesis. *Int J Hyperthermia* 11:315–322.
4. Brizel DM, et al. (1996) Radiation therapy and hyperthermia improve the oxygenation of human soft tissue sarcomas. *Cancer Res* 56:5347–5350.
5. Vujaskovic Z, et al. (2003) Ultrasound guided pO2 measurement of breast cancer reoxygenation after neoadjuvant chemotherapy and hyperthermia treatment. *Int J Hyperthermia* 19:498–506.
6. Jones EL, et al. (2004) Thermochemoradiotherapy improves oxygenation in locally advanced breast cancer. *Clin Cancer Res* 10:4287–4293.
7. Jones EL, et al. (2005) Randomized trial of hyperthermia and radiation for superficial tumors. *J Clin Oncol* 23:3079–3085.
8. Hauck ML, et al. (2006) Phase I trial of doxorubicin-containing low temperature sensitive liposomes in spontaneous canine tumors. *Clin Cancer Res* 12:4004–4010.
9. Ponce AM, Vujaskovic Z, Yuan F, Needham D, Dewhirst MW (2006) Hyperthermia mediated liposomal drug delivery. *Int J Hyperthermia* 22:205–213.
10. Ponce AM, et al. (2007) Magnetic resonance imaging of temperature-sensitive liposome release: Drug dose painting and antitumor effects. *J Natl Cancer Inst* 99: 53–63.
11. Shakil A, Osborn JL, Song CW (1999) Changes in oxygenation status and blood flow in a rat tumor model by mild temperature hyperthermia. *Int J Radiat Oncol Biol Phys* 43: 859–865.
12. Tamulevicius P, Luscher G, Streffer C (1987) Effects on intermediary metabolism in mouse tissues by Ro-03-8799. *Br J Cancer* 56:315–320.
13. Kelleher DK, Engel T, Vaupel PW (1995) Changes in microregional perfusion, oxygenation, ATP and lactate distribution in subcutaneous rat tumours upon water-filtered IR-A hyperthermia. *Int J Hyperthermia* 11:241–255.
14. Streffer C (1985) Metabolic changes during and after hyperthermia. *Int J Hyperthermia* 1:305–319.
15. Vaupel PW, Kelleher DK (2010) Pathophysiological and vascular characteristics of tumours and their importance for hyperthermia: Heterogeneity is the key issue. *Int J Hyperthermia* 26:211–223.
16. Covello KL, Simon MC (2004) HIFs, hypoxia, and vascular development. *Curr Top Dev Biol* 62:37–54.
17. Rankin EB, Giaccia AJ (2008) The role of hypoxia-inducible factors in tumorigenesis. *Cell Death Differ* 15:678–685.
18. Semenza GL (2009) Regulation of cancer cell metabolism by hypoxia-inducible factor 1. *Semin Cancer Biol* 19:12–16.
19. Semenza GL (2003) Targeting HIF-1 for cancer therapy. *Nat Rev Cancer* 3:721–732.
20. Moon EJ, Brizel DM, Chi JT, Dewhirst MW (2007) The potential role of intrinsic hypoxia markers as prognostic variables in cancer. *Antioxid Redox Signal* 9: 1237–1294.
21. Semenza GL (2009) Involvement of oxygen-sensing pathways in physiologic and pathologic erythropoiesis. *Blood* 114:2015–2019.
22. Berra E, et al. (2003) HIF prolyl-hydroxylase 2 is the key oxygen sensor setting low steady-state levels of HIF-1alpha in normoxia. *EMBO J* 22:4082–4090.
23. Forsythe JA, et al. (1996) Activation of vascular endothelial growth factor gene transcription by hypoxia-inducible factor 1. *Mol Cell Biol* 16:4604–4613.
24. Kim JW, Tchernyshyov I, Semenza GL, Dang CV (2006) HIF-1-mediated expression of pyruvate dehydrogenase kinase: A metabolic switch required for cellular adaptation to hypoxia. *Cell Metab* 3:177–185.
25. Jackson IL, Batinic-Haberle I, Sonveaux P, Dewhirst MW, Vujaskovic Z (2006) ROS production and angiogenic regulation by macrophages in response to heat therapy. *Int J Hyperthermia* 22:263–273.
26. Katschinski DM, et al. (2002) Heat induction of the unphosphorylated form of hypoxia-inducible factor-1alpha is dependent on heat shock protein-90 activity. *J Biol Chem* 277:9262–9267.
27. Wartenberg M, et al. (2005) Regulation of the multidrug resistance transporter P-glycoprotein in multicellular prostate tumor spheroids by hyperthermia and reactive oxygen species. *Int J Cancer* 113:229–240.
28. Ferrara N (2004) Vascular endothelial growth factor: Basic science and clinical progress. *Endocr Rev* 25:581–611.
29. Li F, et al. (2007) Regulation of HIF-1alpha stability through S-nitrosylation. *Mol Cell* 26:63–74.
30. Koch CJ (2002) Measurement of absolute oxygen levels in cells and tissues using oxygen sensors and 2-nitroimidazole EF5. *Methods Enzymol* 352:3–31.
31. Cao Y, et al. (2005) Observation of incipient tumor angiogenesis that is independent of hypoxia and hypoxia inducible factor-1 activation. *Cancer Res* 65:5498–5505.
32. Jordan BF, et al. (2003) Nitric oxide-mediated increase in tumor blood flow and oxygenation of tumors implanted in muscles stimulated by electric pulses. *Int J Radiat Oncol Biol Phys* 55:1066–1073.
33. Wang GL, Jiang BH, Rue EA, Semenza GL (1995) Hypoxia-inducible factor 1 is a basic-helix-loop-helix-PAS heterodimer regulated by cellular O2 tension. *Proc Natl Acad Sci USA* 92:5510–5514.
34. Moeller BJ, Cao Y, Li CY, Dewhirst MW (2004) Radiation activates HIF-1 to regulate vascular radiosensitivity in tumors: Role of reoxygenation, free radicals, and stress granules. *Cancer Cell* 5:429–441.
35. Batinić-Haberle I, Rebouças JS, Spasojević I (2010) Superoxide dismutase mimics: Chemistry, pharmacology, and therapeutic potential. *Antioxid Redox Signal* 13: 877–918.
36. Mansfield KD, et al. (2005) Mitochondrial dysfunction resulting from loss of cytochrome c impairs cellular oxygen sensing and hypoxic HIF-alpha activation. *Cell Metab* 1:393–399.
37. Goyal P, et al. (2004) Upregulation of NAD(P)H oxidase 1 in hypoxia activates hypoxia-inducible factor 1 via increase in reactive oxygen species. *Free Radic Biol Med* 36: 1279–1288.
38. Choi JA, et al. (2010) Pro-survival of estrogen receptor-negative breast cancer cells is regulated by a BLT2-reactive oxygen species-linked signaling pathway. *Carcinogenesis* 31:543–551.
39. Segal AW, Abo A (1993) The biochemical basis of the NADPH oxidase of phagocytes. *Trends Biochem Sci* 18:43–47.
40. Adachi Y, et al. (2008) Oncogenic Ras upregulates NADPH oxidase 1 gene expression through MEK-ERK-dependent phosphorylation of GATA-6. *Oncogene* 27:4921–4932.
41. Han SI, et al. (2002) Mild heat shock induces cyclin D1 synthesis through multiple Ras signal pathways. *FEBS Lett* 515:141–145.
42. Shin MH, et al. (2008) Reactive oxygen species produced by NADPH oxidase, xanthine oxidase, and mitochondrial electron transport system mediate heat shock-induced MMP-1 and MMP-9 expression. *Free Radic Biol Med* 44:635–645.
43. Favata MF, et al. (1998) Identification of a novel inhibitor of mitogen-activated protein kinase kinase. *J Biol Chem* 273:18623–18632.
44. Cairns RA, Papandreou I, Sutphin PD, Denko NC (2007) Metabolic targeting of hypoxia and HIF1 in solid tumors can enhance cytotoxic chemotherapy. *Proc Natl Acad Sci USA* 104:9445–9450.
45. Wigfield SM, et al. (2008) PDK-1 regulates lactate production in hypoxia and is associated with poor prognosis in head and neck squamous cancer. *Br J Cancer* 98: 1975–1984.
46. Batinić-Haberle I, Liochev SI, Spasojević I, Fridovich I (1997) A potent superoxide dismutase mimic: Manganese beta-octabromo-meso-tetrakis-(N-methylpyridinium-4-yl) porphyrin. *Arch Biochem Biophys* 343:225–233.
47. Bristow RG, Hill RP (2008) Hypoxia and metabolism: Hypoxia, DNA repair and genetic instability. *Nat Rev Cancer* 8:180–192.
48. Harada H, et al. (2007) Significance of HIF-1-active cells in angiogenesis and radioresistance. *Oncogene* 26:7508–7516.
49. Song X, et al. (2006) Hypoxia-induced resistance to cisplatin and doxorubicin in non-small cell lung cancer is inhibited by silencing of HIF-1alpha gene. *Cancer Chemother Pharmacol* 58:776–784.
50. Brown LM, et al. (2006) Reversing hypoxic cell chemoresistance in vitro using genetic and small molecule approaches targeting hypoxia inducible factor-1. *Mol Pharmacol* 69:411–418.
51. Sullivan R, Paré GC, Frederiksen LJ, Semenza GL, Graham CH (2008) Hypoxia-induced resistance to anticancer drugs is associated with decreased senescence and requires hypoxia-inducible factor-1 activity. *Mol Cancer Ther* 7:1961–1973.
52. Liu L, et al. (2008) Hypoxia-inducible factor-1 alpha contributes to hypoxia-induced chemoresistance in gastric cancer. *Cancer Sci* 99:121–128.
53. Yuan H, et al. (2006) Intertumoral differences in hypoxia selectivity of the PET imaging agent 64Cu(II)-diacetyl-bis(N4-methylthiosemicarbazone). *J Nucl Med* 47: 989–998.
54. Rabbani ZN, et al. (2009) Antiangiogenic action of redox-modulating Mn(III) meso-tetrakis(N-ethylpyridinium-2-yl)porphyrin, MnTE-2-PyP(5+), via suppression of oxidative stress in a mouse model of breast tumor. *Free Radic Biol Med* 47:992–1004.
55. Schroeder T, et al. (2005) Spatial heterogeneity and oxygen dependence of glucose consumption in R3230Ac and fibrosarcomas of the Fischer 344 rat. *Cancer Res* 65: 5163–5171.